THE JOURNAL OF BIOLOGICAL CHEMISTRY VOL. 284, NO. 33, pp. 22173–22183, August 14, 2009

Bile Acid-induced Epidermal Growth Factor Receptor Activation in Quiescent Rat Hepatic Stellate Cells Can Trigger Both Proliferation and Apoptosis[S]

Received for publication, April 7, 2009, and in revised form, June 23, 2009 Published, JBC Papers in Press, June 24, 2009, DOI 10.1074/jbc.M109.005355

Annika Sommerfeld, Roland Reinehr, and Dieter Häussinger[1]

From the Clinic for Gastroenterology, Hepatology, and Infectiology, Heinrich-Heine-University Düsseldorf, D-40225 Düsseldorf, Germany

Bile acids have been reported to induce epidermal growth factor receptor (EGFR) activation and subsequent proliferation of activated hepatic stellate cells (HSC), but the underlying mechanisms and whether quiescent HSC are also a target for bile acid-induced proliferation or apoptosis remained unclear. Therefore, primary rat HSC were cultured for up to 48 h and analyzed for their proliferative/apoptotic responses toward bile acids. Hydrophobic bile acids, *i.e.* taurolithocholate 3-sulfate, taurochenodeoxycholate, and glycochenodeoxycholate, but not taurocholate or tauroursodeoxycholate, induced Yes-dependent EGFR phosphorylation. Simultaneously, hydrophobic bile acids induced phosphorylation of the NADPH oxidase subunit $p47^{phox}$ and formation of reactive oxygen species (ROS). ROS production was sensitive to inhibition of acidic sphingomyelinase, protein kinase Cζ, and NADPH oxidases. All maneuvers which prevented bile acid-induced ROS formation also prevented Yes and subsequent EGFR phosphorylation. Taurolithocholate 3-sulfate-induced EGFR activation was followed by extracellular signal-regulated kinase 1/2, but not c-Jun N-terminal kinase (JNK) activation, and stimulated HSC proliferation. When, however, a JNK signal was induced by coadministration of cycloheximide or hydrogen peroxide (H_2O_2), activated EGFR associated with CD95 and triggered EGFR-mediated CD95-tyrosine phosphorylation and subsequent formation of the death-inducing signaling complex. In conclusion, hydrophobic bile acids lead to a NADPH oxidase-driven ROS generation followed by a Yes-mediated EGFR activation in quiescent primary rat HSC. This proliferative signal shifts to an apoptotic signal when a JNK signal simultaneously comes into play.

Hydrophobic bile acids play a major role in the pathogenesis of cholestatic liver disease and are potent inducers of hepatocyte apoptosis by triggering a ligand-independent activation of the CD95[2] death receptor (1–5). The underlying molecular mechanisms are complex and involve a Yes-dependent, but ligand-independent activation of the epidermal growth factor receptor (EGFR), which catalyzes CD95-tyrosine phosphorylation as a prerequisite for CD95 oligomerization, formation of the death-inducing signaling complex (DISC), and apoptosis induction (6, 7). Bile acids also activate EGFR in cholangiocytes (8) and activated hepatic stellate cells (HSC) (9), however, the mechanisms underlying bile acid-induced EGFR activation in HSC remained unclear (9). Surprisingly, bile acid-induced EGFR activation in HSC does not trigger apoptosis but results in a stimulation of cell proliferation (9). The behavior of quiescent HSC toward CD95 ligand (CD95L) is also unusual. CD95L, which is a potent inducer of hepatocyte apoptosis (10–12), triggers activation of the EGFR in quiescent HSC, stimulates HSC proliferation, and simultaneously inhibits CD95-dependent death signaling through CD95-tyrosine nitration (13). Similar observations were made with other death receptor ligands, *i.e.* tumor necrosis factor-α (TNF-α) and TNF-related apoptosis-inducing ligand (TRAIL) (13). The mitogenic action of CD95L in quiescent, 1–2-day cultured HSC is because of a c-Src-dependent shedding of EGF and subsequent auto/paracrine activation of the EGFR (13). This unusual behavior of quiescent HSC toward death receptor ligands may relate to the recent findings that quiescent HSC might represent a stem/progenitor cell compartment in the liver with a capacity to differentiate not only into myofibroblasts but also toward hepatocyte- and endothelial-like cells (14). Thus, stimulation of HSC proliferation and resistance toward apoptosis in the hostile cytokine milieu accompanying liver injury may help HSC to play their role in liver regeneration. During cholestatic liver injury quiescent HSC are exposed to increased concentrations of circulating bile acids, but it is not known whether this may lead to HSC proliferation (as shown for activated HSC) (9), HSC apoptosis (as shown for hepatocytes) (1–7), or both of them. Therefore, the aim of the current study was (*a*) to identify the molecular mechanisms underlying bile acid-induced EGFR activation and (*b*) to elucidate whether bile acid-induced signaling can couple to both cell proliferation and cell death in quiescent HSC.

[S] The on-line version of this article (available at http://www.jbc.org) contains supplemental Figs. 1–5.

[1] To whom correspondence should be addressed: Universitätsklinikum Düsseldorf, Klinik für Gastroenterologie, Hepatologie und Infektiologie, Moorenstrasse 5, D-40225 Düsseldorf, Germany. Tel.: 49-2118117569; Fax: 49-2118118838; E-mail: haeussin@uni-duesseldorf.de.

[2] The abbreviations used are: CD95, Fas, APO-1, CD95 receptor; BrdUrd, bromodeoxyuridine; CD95L, CD95 ligand; CHX, cycloheximide; CM-H_2DCFDA, 5-(and-6-)-chloromethyl-2′,7′-dichlorodihydrofluorescein diacetate; EGFR, epidermal growth factor (EGR) receptor; Erk, extracellular signal-regulated kinase; FADD, Fas-associated death domain; Gadd45β, growth arrest and DNA damage-inducible gene 45β; GCDC, glycochenodeoxycholate; HSC, hepatic stellate cells; JNK, c-Jun N-terminal kinase; $p38^{MAPK}$, p38 mitogen-activated protein kinase; PKCζ inhibitor, cell-permeable myristoylated PKCζ pseudosubstrate; ROS, reactive oxygen species; SMA, smooth muscle actin; TC, taurocholate; TCDC, taurochenodeoxycholate; TLCS, taurolithocholate 3-sulfate; TUDC, tauroursodeoxycholate; TUNEL, TdT-mediated X-dUTP nick end labeling; DISC, death-inducing signaling complex.

The present study shows that cholestatic bile acids trigger a rapid NADPH oxidase activation in quiescent HSC, which leads to a Yes-mediated EGFR phosphorylation and HSC proliferation. In contrast to hepatocytes, hydrophobic bile acids do not induce a JNK signal in HSC. However, when JNK activation is induced by coadministration of either cycloheximide (CHX) or hydrogen peroxide (H_2O_2), the bile acid-induced mitogenic signal is shifted to an apoptotic one.

EXPERIMENTAL PROCEDURES

Materials—The materials used were purchased as follows: Dulbecco's modified Eagle's medium and fetal calf serum from PAA Laboratories (Linz, Austria); taurolithocholate 3-sulfate (TLCS), taurochenodeoxycholate (TCDC), taurocholate (TC), tauroursodeoxycholate (TUDC), glycochenodeoxycholate (GCDC), epidermal growth factor (EGF), CHX, *N*-acetylcysteine, desipramine, and AY9944 from Sigma-Aldrich; penicillin/streptomycin from Biochrom (Berlin, Germany); nycodenz from Nycomed (Oslo, Norway); Pronase from Merck; desoxyribonuclease I and collagenases from Roche Applied Science; Fluoresbrite plain YG 1-μm microspheres from Polyscience (Worrington, PA); TUNEL assay from Roche Diagnostics; GM6001 (galardin), apocynin, myr-PKCζ-pseudosubstrate inhibitor (PKCζ-inhibitor), chelerythrine, AG1478, SU6656, and PP-2 from Calbiochem; diphenyleneiodonium chloride from Biomol (Hamburg, Germany); CM-H_2DCFDA from Molecular Probes (Eugene, OR). L-JNKI-1, SB203580, and soluble CD95L, which was always employed with a 10-fold amount of enhancer protein as provided by the supplier, were obtained from Alexis Biochemicals (San Diego, CA).

The antibodies used were purchased as follows: mouse anti-γ-tubulin and mouse anti-α-smooth muscle actin (αSMA) antibodies from Sigma-Aldrich, rabbit anti-p47^{phox} (immunoprecipitation (IP)), rabbit anti-Yes (IP), rabbit anti-Fyn (IP), rabbit anti-EGFR (IP), rabbit anti-p38^{MAPK}, rabbit anti-CD95 (IP, C-20; Western blot, M-20), rabbit anti-FADD, and mouse anti-caspase 8 antibodies from Santa Cruz Biotechnology (Santa Cruz, CA); rabbit anti-phospho-Src family Tyr^{418}, mouse anti-phospho-Erk1/2, and rabbit anti-phospho-EGFR (EGFR-Tyr(P)^{1045}) antibodies from Cell Signaling (Beverly, MA); mouse anti-phospho-c-Src-Tyr^{418} and mouse anti-3′-nitrotyrosine antibodies from Calbiochem; rabbit anti-phospho-p38^{MAPK}, rabbit anti-phospho-JNK1/2, rabbit anti-phospho-EGFR antibodies (EGFR Tyr(P)^{845} and Tyr(P)^{1173}), and rabbit anti-c-Src from BioSource Int. (Camarillo, CA); rabbit anti-Yes (Western blot (WB)), rabbit anti-Fyn (WB), sheep-anti-EGFR (WB), rabbit anti-p47^{phox} (WB), rabbit anti-Erk1/2, and mouse anti-phosphotyrosine antibodies from Upstate Biotechnology (Lake Placid, NY); mouse anti-phosphoserine (clone16B4) antibody from Biomol (Hamburg, Germany); rabbit anti-JNK1/2 from BD Pharmingen. Protein A/G-agarose was obtained from Santa Cruz, horseradish peroxidase-conjugated anti-mouse IgG and Bio-Rad protein assay was from Bio-Rad, and the enhanced chemiluminescence detection kit was from Amersham Biosciences. All other chemicals were from Merck at the highest quality available.

Cell Preparation and Culture—HSC were isolated from male Wistar rats as described (13, 15). After isolation HSC were identified by their typical morphology, the vitamin A droplet-dependent autofluorescence, and by their inability to phagocytose latex beads. The yield of HSC was about 30×10^6 cells with a purity greater than 95% as assessed 24 h after seeding. HSC were plated on 6-well culture plates (Falcon, Heidelberg, Germany) and cultured in Dulbecco's modified Eagle's medium supplemented with 10% fetal calf serum, 13 mmol/liter glucose, 4 mmol/liter glutamine, and antibiotics at 37 °C in a 5% CO_2 atmosphere (13, 15). Unless otherwise indicated, all experiments reported throughout this manuscript were performed in primary rat HSC, which did not exceed 48 h of culture, thereby representing a "quiescent" phenotype. In contrast, primary rat HSC cultured for 10–14 days were taken to investigate an "activated" phenotype.

Western Blot Analysis—After the respective incubations, medium was removed, and the cells were washed briefly with phosphate-buffered saline and lysed immediately. They were harvested in 1% SDS containing 62.5 mmol/liter Tris-HCl, pH 6.8. The lysates were centrifuged at $1000 \times g$ for 3 min at 4 °C, and aliquots were taken for protein determination using the Bio-Rad protein assay. Samples were transferred to SDS/PAGE, and proteins were blotted to nitrocellulose membranes using a semidry transfer apparatus (GE Healthcare) (12, 13). Blots were blocked for 2 h in 5% (w/v) bovine serum albumin-containing 20 mmol/liter Tris, pH 7.5, 150 mmol/liter NaCl, and 0.1% Tween 20 (TBS-T), and then incubated at 4 °C overnight with the respective antibody. After washing with TBS-T and incubation with horseradish peroxidase-coupled anti-mouse, anti-sheep, or anti-rabbit IgG antibody (all diluted 1:10,000) at room temperature for 2 h, the blots were washed extensively and developed using enhanced chemiluminescent detection (Amersham Biosciences). Blots were exposed to Kodak X-Omat AR-5 film (Eastman Kodak Co.).

Immunoprecipitation—Cells were harvested in lysis buffer as published (13). Equal protein amounts (200 μg) of each sample were incubated for 2 h at 4 °C with rabbit anti-CD95, rabbit anti-EGFR, rabbit anti-p47^{phox}, rabbit anti-Yes antibody, or rabbit anti-Fyn-antibodies (all Santa Cruz; dilution 1:100) to immunoprecipitate CD95, EGFR, p47^{phox}, Yes, or Fyn. Then 10 μl of protein A- and 10 μl of protein-G-agarose were added and incubated at 4 °C overnight. Immunoprecipitates were washed 3 times and then transferred for Western blot analysis (13). Activation of p47^{phox} by serine phosphorylation was detected using anti-phosphoserine antibodies (16). Anti-phospho-Src family Tyr^{418} antibodies were used to detect activating phosphorylation of Yes or Fyn (17) and anti-phosphotyrosine antibodies were used to detect EGFR-tyrosine phosphorylation in the respective immunoprecipitates. FADD and caspase 8 association, tyrosine phosphorylation, or tyrosine nitration of the immunoprecipitated CD95 samples were detected by Western blot analysis.

Detection of HSC Proliferation—HSC proliferation was measured using a colorimetric BrdUrd cell proliferation assay ((+)-5-bromo-2′-deoxyuridine-ELISA, Roche Diagnostics). Therefore, HSC were cultured in flat-bottomed 96-well microtiter plates for up to 48 h. The culture medium was removed and replaced by Dulbecco's modified Eagle's medium containing BrdUrd. For the respective samples, BrdUrd incorporation

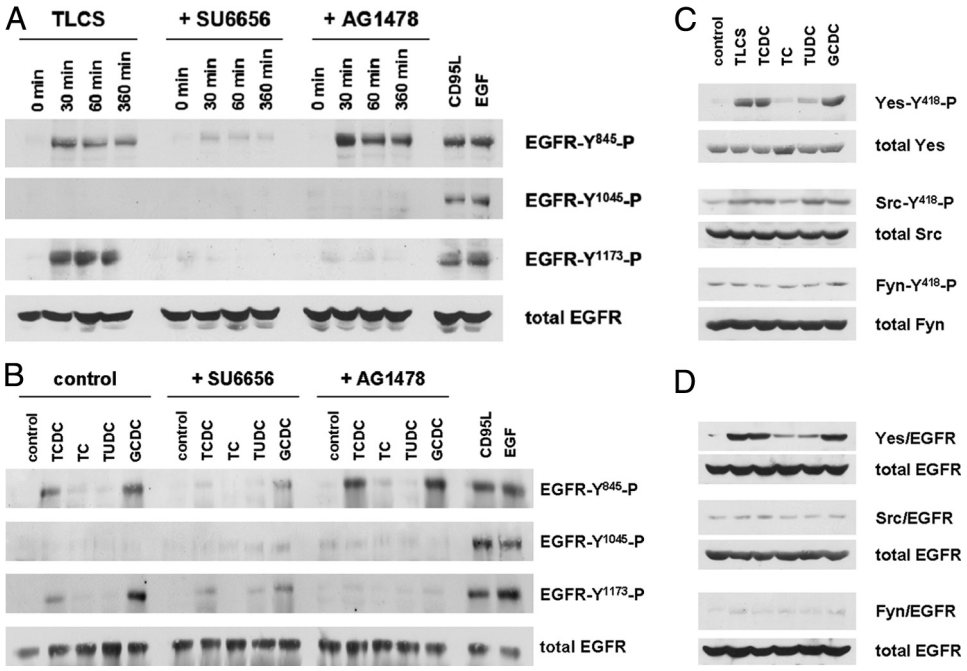

FIGURE 1. **Bile acid-induced EGFR phosphorylation in quiescent HSC.** Quiescent HSC were exposed to TLCS (100 μmol/liter) for the time periods indicated or for 30 min to either TCDC, TC, TUDC, or GCDC (100 μmol/liter), CD95L (100 ng/ml), or EGF (50 ng/ml). When indicated, SU6656 (10 μmol/liter), an inhibitor of Src kinases (Yes, Fyn, and c-Src) (36), or AG1478 (5 μmol/liter), an EGFR-tyrosine kinase inhibitor (32), were added 30 min before TLCS addition. Phosphorylation of EGFR-tyrosine residues Tyr^{845}, Tyr^{1045}, and Tyr^{1173} were analyzed by Western blot using phospho-specific antibodies. Total EGFR served as loading control (*A* and *B*). Yes, c-Src, and Fyn were analyzed for activating phosphorylation at position Tyr^{418} by either immunoprecipitation (Yes, Fyn) or by use of a phospho-specific antibody (c-Src) as given under "Experimental Procedures." Total Yes, c-Src, and Fyn served as respective loading controls (*C*). EGFR was immunoprecipitated and subsequently detected for Yes, c-Src, or Fyn by Western blot. Total EGFR served as loading control (*D*). Representative experiments from a series of three independent experiments are shown. *A*, in line with earlier studies (13), CD95L and EGF induced EGFR-tyrosine phosphorylation at positions Tyr^{845}, Tyr^{1045}, and Tyr^{1173}. In contrast, TLCS induced EGFR phosphorylation at positions Tyr^{845} and Tyr^{1173} only. AG1478 prevented EGFR autophosphorylation at position Tyr^{1173} but did not prevent TLCS-induced phosphorylation at position Tyr^{845}. This may suggest that TLCS leads to a Src family kinase-mediated EGFR activation at position Tyr^{845}, which is followed by EGFR-mediated autophosphorylation at position Tyr^{1173}. *B*, like TLCS, the pro-apoptotic bile acids TCDC and GCDC, but not TC and TUDC, also trigger EGFR phosphorylation. *C*, TLCS, TCDC, and GCDC induced phosphorylation of Yes but not of Fyn. Only a weak c-Src phosphorylation was detectable. TC was ineffective, and TUDC induced only a weak Yes and c-Src phosphorylation. For statistical analysis see supplemental Fig. 1. Representative experiments from a series of three independent experiments are shown. *D*, TLCS, TCDC, and GCDC, but not TC and TUDC, trigger an association of Yes (but not of Fyn or c-Src) with the EGFR. For time courses of TLCS-induced Yes/EGFR association, see supplemental Fig. 2.

was determined according to the manufacturer's recommendations. In addition, cell number was counted using a Neubauer chamber.

Detection of Reactive Oxygen Species (ROS)—Cells were seeded and cultured as indicated and then incubated with phosphate-buffered saline containing 5 μmol/liter CM-H_2DCFDA for 30 min at 37 °C and 5% CO_2. To detect ROS generation, CM-H_2DCFDA-loaded cells were supplemented again with culture medium and then exposed to the respective bile acids and inhibitors for the indicated time period. Then cells were washed briefly using ice-cold phosphate-buffered saline and lysed in 0.1% Triton X-100 (v/v) dissolved in aqua bidest (extrapure water). Lysates were centrifuged immediately (10,000 $\times$ *g*, 4 °C, 1min), and fluorescence of the supernatant was measured at 515–565 nm using a luminescence spectrometer LS-5B (PerkinElmer Life Sciences) at 488-nm excitation wavelength. Fluorescence of untreated control cells was arbitrarily set to 1.

Detection of Apoptosis—Terminal deoxynucleotidyltransferase-mediated X-dUTP-nick-end-labeling of fluorescein isothiocyanate-conjugated deoxyuridine trisphosphate (TUNEL)-technique was performed as described (12, 13). The number of apoptotic cells was determined by counting the percentage of fluorescein-positive cells. At least 100 cells from three different cell preparations were counted for each condition. Cells were visualized on an Axioskop (Zeiss).

Reverse Transcription-PCR—Primary HSC and primary rat hepatocytes (parenchymal cells) were detected for Gadd45β-mRNA expression by reverse transcription-PCR as described recently (13) using the following primers for Gadd45β (sense-5′-GAA AGC CTC GGA CAC TTC TG-3′ and antisense-5′-GCC TGA TAC CCT GAC GAT GT-3′) and β-actin (sense-5′-GCC CTA GAC TTC GAG CAA GA-3′ and antisense-5′-CAG TGA GGC CAG GAT AGA GC-3′).

Statistics—Results from at least three independent experiments are expressed as the means ± S.E. (S.E.). *n* refers to the number of independent experiments. Results were analyzed using Student's *t* test; $p < 0.05$ was considered statistically significant.

RESULTS

Bile Acid-induced Phosphorylation of the EGFR in Quiescent HSC—HSC in culture for 24–48 h were considered as quiescent because they contained vitamin A-containing fat droplets and expressed glial fibrillary acidic protein and desmin but no or very little αSMA (13, 14). After 7–14 days of culture, the cells had lost their lipid droplets and strongly expressed αSMA, reflecting their transformation into myofibroblasts (18–20).

TLCS induced within 30 min of phosphorylation of the EGFR in quiescent HSC, which involved the tyrosine residues Tyr^{845} and Tyr^{1173} but not tyrosine residue Tyr^{1045} (Fig. 1*A*). Similar findings were obtained with other pro-apoptotic bile acids, such as GCDC and TCDC, whereas no EGFR phosphorylation was observed in response to TC or TUDC (Fig. 1*B*). Tyr^{845} is a known Src kinase phosphorylation site (21), whereas Tyr^{1173} phosphorylation indicates activation and autophosphorylation of the EGFR (22). The failure of TLCS and other pro-apoptotic bile acids to induce EGFR phosphorylation at position Tyr^{1045} (Fig. 1, *A* and *B*) suggests that TLCS does not activate the EGFR in a ligand-dependent auto/paracrine way, as it was recently shown for CD95L-induced and EGF-dependent EGFR activation in quiescent HSC (Fig. 1, *A* and *B*) (13). In line with this,

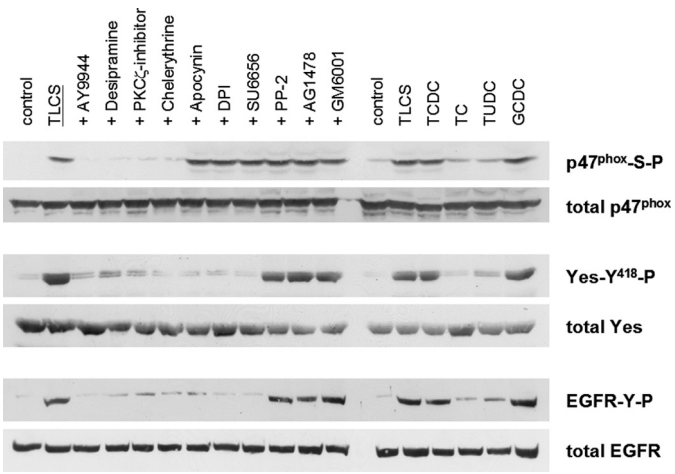

FIGURE 2. **Pharmacological characterization of bile acid-induced p47^{phox}, Yes, and EGFR phosphorylation in quiescent HSC.** Quiescent HSC were exposed to either TLCS, TCDC, TC, TUDC, or GCDC (100 μmol/liter, each) for 30 min. When indicated, AY9944 (5 μmol/liter), desipramine (5 μmol/liter), PKCζ inhibitor (100 μmol/liter), chelerythrine (20 μmol/liter), apocynin (300 μmol/liter), diphenyleneiodonium (*DPI*, 10 μmol/liter), SU6656 (10 μmol/liter), PP-2 (10 μmol/liter), or AG1478 (5μmol/liter) were preincubated for 30 min, whereas the broad-spectrum matrix metalloproteinase inhibitor GM6001 (25 μmol/liter) (8) was added 16 h before TLCS addition. p47^{phox}, Yes, and EGFR were immunoprecipitated and then analyzed for activating p47^{phox} -serine phosphorylation, Yes-Tyr^{418} phosphorylation, and EGFR-tyrosine phosphorylation by phospho-specific antibodies as described under "Experimental Procedures." Total p47^{phox}, Yes, and EGFR served as respective loading controls. As in hepatocytes (23), TLCS-induced activation of the NADPH oxidase subunit p47^{phox} as well as Yes and EGFR phosphorylation was sensitive to inhibitors of sphingomyelinases (AY9944, desipramine) or protein kinase Cζ (PKCζ inhibitory pseudosubstrate, chelerythrine). In addition, TLCS-induced Yes phosphorylation was sensitive to inhibition of NADPH oxidases (apocynin, diphenyleneiodonium chloride). In line with the literature (7), Yes phosphorylation was also sensitive to SU6656 but not to PP-2. All compounds which inhibited NADPH oxidases and subsequent Yes activation also blocked EGFR-tyrosine phosphorylation. The data suggest a NADPH oxidase- and Yes-dependent EGFR transactivation. GM6001, which has been reported to inhibit bile acid-induced EGFR activation in cholangiocytes (8) or CD95L-induced EGFR activation in quiescent HSC (13), did not affect TLCS-induced EGFR phosphorylation in quiescent HSC. Similar effects were obtained with TCDC and GCDC but not with TC or TUDC. Representative experiments from a series of three independent experiments are shown.

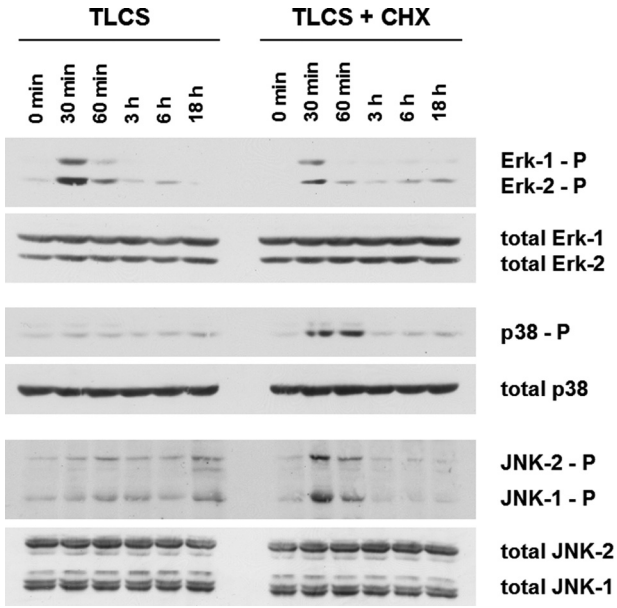

FIGURE 3. **Bile acid-induced activation of mitogen-activated protein kinases in quiescent HSC.** Quiescent HSC were exposed to TLCS (100 μmol/liter) for the time periods indicated. When indicated, CHX (0.5 μmol/liter) was added simultaneously with TLCS. Phosphorylation of Erk1/2, p38^{MAPK}, and JNK1/2 was analyzed by Western blot using phospho-specific antibodies. Total Erk1/2, p38^{MAPK}, and JNK1/2 served as loading controls. TLCS induced within 30 min a phosphorylation of Erk1/2 but only a weak JNK signal, and no p38^{MAPK} phosphorylation became detectable. Coadministration of TLCS/CHX resulted in a substantial JNK1/2 and p38^{MAPK} phosphorylation, whereas the Erk signal was suppressed. For statistical analysis see supplemental Fig. 4. Representative experiments from a series of six independent experiments are shown.

neither the shedding inhibitor GM6001 nor neutralizing EGF antibodies were able to block TLCS-induced EGFR phosphorylation (not shown). Because EGFR-Tyr^{845} is a known substrate for Src family kinases (17, 21) and Yes mediates bile acid-induced EGFR activation in rat hepatocytes (7), effects of different bile acids on the phosphorylation of Src kinase family members were examined in quiescent HSC.

As shown in Fig. 1*C*, hydrophobic bile acids, but not TC or TUDC, induced within 30 min a substantial Yes-, but no Fyn phosphorylation, whereas c-Src phosphorylation was only weak (for statistical analysis, see supplemental Fig. 1). EGFR transactivation by Src family kinases requires their physical association with EGFR. As shown in Fig. 1*D*, hydrophobic bile acids, but not TC or TUDC, triggered an association of the EGFR with Yes but not with Fyn or c-Src. TLCS-induced Yes/EGFR association lasted for up to 6 h, whereas TC failed to induce Yes/EGFR association within this time frame (see supplemental Fig. 2). These data suggest that TLCS, TCDC, and GCDC activate the Src family kinase Yes, which associates with the EGFR and catalyzes EGFR activation. In line with this, inhibition of Yes by SU6656 abolished TLCS-induced EGFR phosphorylation in quiescent HSC, whereas PP-2 (an inhibitor of c-Src but not of Yes) failed to do so (Fig. 2). Furthermore, the EGFR-tyrosine kinase inhibitor AG1478 had no effect on bile acid-induced Yes phosphorylation, indicating that EGFR phosphorylation is located downstream of Yes activation (Fig. 2).

Hydrophobic Bile Acids Induce Oxidative Stress in Quiescent HSC through Activation of NADPH Oxidases—Hydrophobic bile acids, *i.e.* TLCS, GCDC, and TCDC, were shown to activate NADPH oxidase isoenzymes in rat hepatocytes via phosphorylation of the regulatory subunit p47^{phox} (23), and the resulting formation of ROS was identified as a trigger for Yes activation (7, 23). Also, in quiescent HSC, TLCS, TCDC, and GCDC, but not TC or TUDC, induced serine phosphorylation of p47^{phox} (Fig. 2), which was sensitive to inhibition of acidic sphingomyelinase (AY9944, desipramine) or PKCζ inhibitor (chelerythrine), respectively (Fig. 2). This inhibitor profile resembles that of bile acid-induced NADPH oxidase activation in rat hepatocytes (7, 23). Bile acid-induced p47^{phox}-serine phosphorylation was accompanied by a stimulation of ROS formation as detected by dichlorodihydrofluorescein diacetate fluorescence (see supplemental Fig. 3). TLCS-induced ROS formation in quiescent HSC was not only sensitive to inhibitors of NADPH oxidases (*e.g.* apocynin, diphenyleneiodonium chloride) but also to inhibition of acidic sphingomyelinase by AY9944 or of protein kinase Cζ using a PKCζ inhibitory pseudosubstrate (see supplemental Fig. 3*B*). These findings suggest that hydrophobic bile acids induce oxidative stress through activation of NADPH oxidases in a sphingomyelinase- and PKCζ-dependent manner.

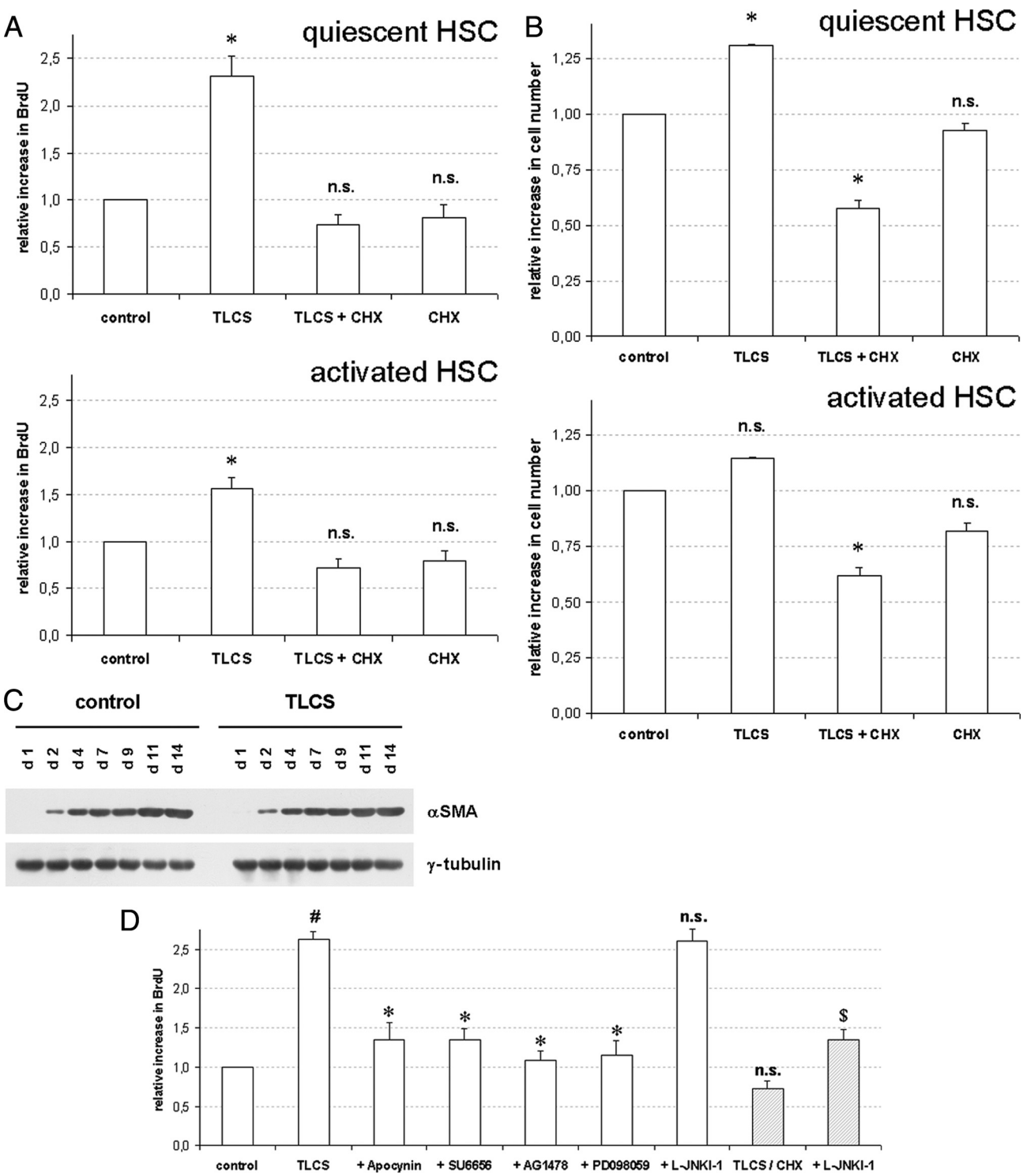

FIGURE 4. **Bile acid-induced BrdUrd incorporation, proliferation, and apoptosis in primary rat HSC.** Quiescent (*A–D*) or activated HSC (*A* and *B*) were exposed to either TLCS (100 μmol/liter), CHX (0.5 μmol/liter), or TLCS/CHX for the time periods indicated. Cells were then tested for BrdUrd incorporation (*A* and *D*) or proliferation (*B*) as described under "Experimental Procedures." If indicated, apocynin (300 μmol/liter), SU6656 (10 μmol/liter), AG1478 (5 μmol/liter), PD098059 (5 μmol/liter), or JNK inhibitor (L-JNKI-1, 5 μmol/liter) were added 30 min before TLCS or TLCS/CHX addition, respectively. In another set of experiments HSC were exposed to either control medium or TLCS for the time periods indicated (*C*) and then tested for α-smooth muscle actin (α*SMA*) expression as a surrogate marker for HSC transdifferentiation to myofibroblast-like cells by Western blot. γ-Tubulin served as the loading control. Representative experiments from a series of three independent experiments are shown. *A*, BrdUrd incorporation. TLCS stimulated BrdUrd incorporation in both quiescent and activated HSC within 48 h. The *asterisk* denotes statistical significance compared with control ($p < 0.05$); *B*, proliferation. The cell number also increased significantly within 48 h of TLCS addition in quiescent HSC but did not reach statistical significance in activated HSC. In contrast, coadministration of TLCS and CHX significantly decreased total cell number. The *asterisk* (*) denotes statistical significance compared with control ($p < 0.05$). *C*, HSC transdifferentiation to myofibroblast. Culture-dependent αSMA-expression was not affected by TLCS. *D*, Inhibitor profile. TLCS-induced increase in BrdUrd incorporation was sensitive to inhibition of NADPH oxidases, Yes-, EGFR-tyrosine kinase activity and Erk but not to JNK-inhibition. In contrast, upon TLCS/CHX coadministration, the otherwise observed TLCS-induced increase in BrdUrd incorporation did not occur but was reinstituted upon simultaneous JNK-inhibition. # denotes statistical significance compared with control ($p < 0.05$); */$ denotes significant inhibition compared with TLCS or TLCS/CHX, respectively ($p < 0.05$); *n.s.*, (not significant, $p > 0.05$).

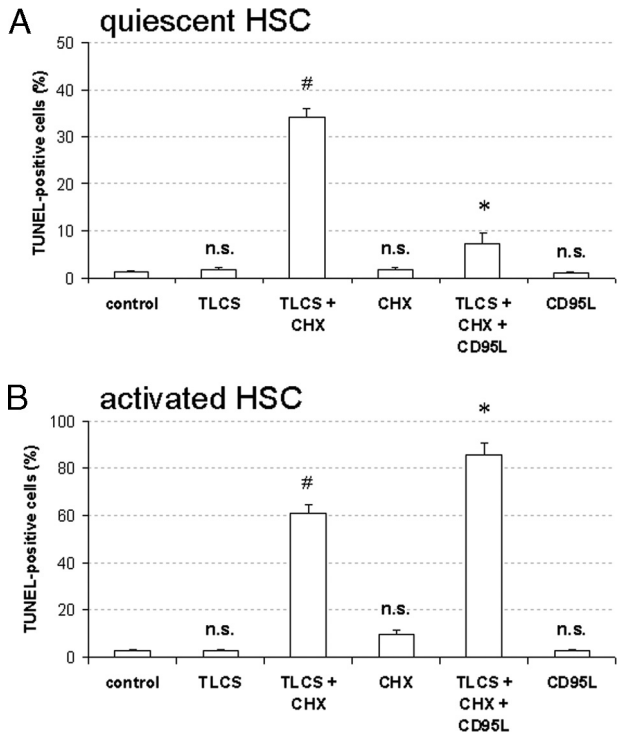

FIGURE 5. **Bile acid-induced apoptosis in quiescent HSC.** Quiescent (*A* and *B*) or activated HSC (*A*) were either exposed to TLCS (100 μmol/liter), CHX (0.5 μmol/liter), or both TLCS and CHX for 24 h. In another set of experiments CD95L (100 ng/ml) was administered together with TLCS/CHX for 24 h. If indicated, AY9944 (5 μmol/liter), PKCζ inhibitor (100 μmol/liter), apocynin (300 μmol/liter), SU6656 (10 μmol/liter), AG1478 (5 μmol/liter), PD098059 (5 μmol/liter), or JNK inhibitor (L-JNKI-1, 5 μmol/liter) were added 30 min before TLCS/CHX coadministration. The percentage of apoptotic cells was detected using TUNEL staining as described under "Experimental Procedures." *A*, apoptosis. Coadministration of TLCS and CHX induced within 24 h a significant increase in apoptotic cells with respect to positive TUNEL staining in both quiescent and activated HSC, whereas treatment with either TLCS or CHX failed to induce apoptosis in those cells. Whereas CD95L inhibited TLCS/CHX-induced apoptotic cell death in quiescent HSC, the number of apoptotic cells even increased in activated HSC. This is explained by CD95L-induced CD95-tyrosine nitration, which induces apoptosis resistance in quiescent HSC, whereas in activated HSC apoptosis is induced by CD95L/CHX (see Fig. 7*B*) (13). # denotes statistical significance compared with control ($p < 0.05$); *n.s.* (not significant) compared with control ($p > 0.05$); * denotes statistical significance compared with TLCS/CHX ($p < 0.05$). *B*, inhibitor profile. TLCS/CHX-induced apoptosis was sensitive to inhibitors of sphingomyelinases, PKCζ, NADPH oxidases, Yes, EGFR-tyrosine kinase activity and JNK, whereas Erk inhibition was ineffective. # denotes statistical significance compared with control ($p < 0.05$); * denotes significant inhibition compared with TLCS/CHX ($p < 0.05$); *n.s.* (not significant) compared with TLCS/CHX ($p > 0.05$).

Interestingly, TLCS-induced ROS formation was transient and less pronounced in quiescent HSC when compared with hepatocytes (see supplemental Fig. 3).

Bile Acid-induced Oxidative Stress Triggers Yes-mediated Phosphorylation of the EGFR in Quiescent HSC—Bile acid-induced oxidative stress triggers Yes activation in rat hepatocytes, probably through inhibition of Yes kinase-regulating phosphatases (7). NADPH oxidase activation apparently also accounts for bile acid-induced Yes activation in quiescent HSC, because Yes phosphorylation in response to TLCS, TCDC, or GCDC was not only sensitive to inhibitors of NADPH oxidases (apocynin, diphenyleneiodonium chloride) but also to inhibitors of acidic sphingomyelinase (AY9944, desipramine) or PKCζ (PKCζ inhibitor, chelerythrine) (Fig. 2). All maneuvers which prevented $p47^{phox}$ and Yes activation, *i.e.* inhibition of acidic sphingomyelinase, PKCζ, NADPH oxidases, and Yes, also prevented bile acid-induced EGFR phosphorylation (Fig. 2). The findings suggest that in quiescent HSC hydrophobic bile acids induce an acidic sphingomyelinase-, PKCζ-, and NADPH oxidase-dependent ROS formation (see supplemental Fig. 3), which further results in Yes activation. Yes then associates with the EGFR (Fig. 1*D*) and mediates an activating EGFR phosphorylation at tyrosine Tyr^{845} followed by EGFR autophosphorylation at Tyr^{1173} (Figs. 1 and 2).

Hydrophobic Bile Acids Stimulate Proliferation of Quiescent HSC—Whereas bile acid-induced EGFR activation in hepatocytes triggers activation of the CD95 system and subsequent hepatocyte apoptosis (5–7), bile acids were reported to stimulate proliferation in passaged cultures of activated HSC after serum-free incubations (9). In HSC cultured for 24–48 h only, TLCS also induced activation of Erk1/2, but not of $p38^{MAPK}$ or JNK1/2 (Fig. 3), and significantly increased BrdUrd incorporation (Fig. 4*A*) and cell number (Fig. 4*B*), whereas TLCS-induced proliferation in activated HSC cultured for 14 days was only small (Figs. 4, *A* and *B*). This suggests that TLCS acts as a mitogen and induces proliferation in quiescent HSC. However, TLCS did not accelerate HSC transformation to myofibroblast-like cells with respect to α-smooth muscle actin expression (Fig. 4*C*).

HSC proliferation in response to TLCS was sensitive to inhibition of NADPH oxidases, Yes-, EGFR-tyrosine kinase activity or Erk1/2 by apocynin, SU6656, AG1478, and PD098059, respectively. On the other hand, inhibition of JNK1/2 by L-JNKI-1 did not affect the mitogenic effect of TLCS (Fig. 4*D*).

Cycloheximide Switches Bile Acid-induced Proliferation toward Apoptosis—In line with its mitogenic effect, TLCS did not increase the number of apoptotic cells, as detected by TUNEL staining (Fig. 5*A*). When, however, CHX, which by itself did not induce apoptosis (Fig. 5*A*), was added together with TLCS, HSC apoptosis was induced, and the proliferative effect of TLCS had completely disappeared (Fig. 4, *A* and *B*). Interestingly, coadministration of CD95L together with TLCS/CHX prevented apoptotic cell death in quiescent HSC, whereas, in contrast, apoptosis was even increased in activated HSC (Fig. 5*A*). This is probably explained by the recent demonstration that CD95L induces apoptosis resistance through CD95-tyrosine nitration in quiescent HSC (13). Such a response was not found in activated HSC, and here CD95L/CHX coadministration was shown to induce apoptosis (13).

Coadministration of TLCS/CHX had no effect on TLCS-induced EGFR activation (Figs. 6*A* and 7*A*) but induced a marked JNK1/2 phosphorylation compared with TLCS alone, whereas the TLCS-induced Erk1/2 phosphorylation was strongly blunted in the presence of CHX (Fig. 3, for statistical analysis, see supplemental Fig. 4). CHX alone induced JNK1/2 and $p38^{MAPK}$ phosphorylation, whereas almost no Erk1/2 phosphorylation was detectable (see supplemental Fig. 5*A*). As for control, inhibition of $p38^{MAPK}$ by SB203580 did not prevent TLCS/CHX-induced JNK1/2 or CD95 activation, respectively (see supplemental Fig. 5*B*), suggesting that CHX-induced $p38^{MAPK}$ activation is probably not involved in TLCS/CHX-induced activation of the CD95 machinery.

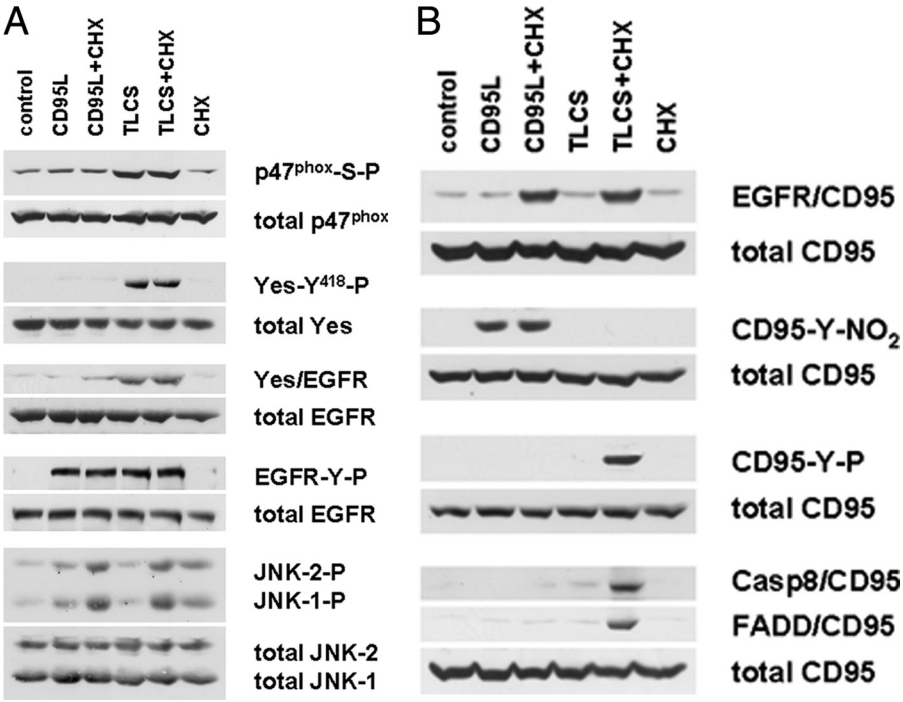

FIGURE 6. **Bile acid-induced activation of the CD95 system in quiescent HSC.** Quiescent HSC were exposed to TLCS (100 μmol/liter), CHX (0.5 μmol/liter) or CD95L (100 ng/ml), or a combination of TLCS/CHX or CD95L/CHX. Activation of $p47^{phox}$, Yes, EGFR, JNK, and CD95 as well as CD95-tyrosine nitration and DISC formation (*i.e.* association of FADD and caspase 8 to CD95) were detected as described under "Experimental Procedures." $p47^{phox}$-serine phosphorylation, Yes-tyrosine phosphorylation, Yes/EGFR association, EGFR-tyrosine phosphorylation, and JNK1/2 phosphorylation were all detected after 30 min, CD95/EGFR association, CD95-tyrosine phosphorylation (CD95-Y-P), and CD95-tyrosine nitration (CD95-Y-NO_2) were detected after 60 min, whereas DISC formation was determined after 3 h of the respective incubations. Total $p47^{phox}$, Yes, EGFR, CD95, and JNK1/2 served as loading controls. Representative experiments from a series of three independent experiments are shown. *A*, EGFR activation. TLCS induced a $p47^{phox}$-serine phosphorylation that was followed by Yes activation, Yes/EGFR association, and subsequent EGFR transactivation, whereas CD95L failed to induce $p47^{phox}$ or Yes activation. Neither CD95L and TLCS induced a marked JNK activation, which only occurred if CD95L or TLCS, respectively, was coadministered together with CHX. *B*, CD95 activation. Again, both CD95L and TLCS failed to induce a CD95/EGFR association, which has been reported to depend on a pronounced JNK activation (13, 24). Whereas CD95L induced CD95-tyrosine nitration in line with earlier findings (13), no CD95-tyrosine phosphorylation and subsequent DISC formation occurred even when coadministered together with CHX (13). In contrast, as TLCS did not induce a protective CD95-tyrosine nitration (13, 25), upon TLCS/CHX coadministration CD95-tyrosine phosphorylation and subsequent DISC formation became detectable.

In the presence of TLCS/CHX, EGFR associated with CD95, which was recently shown to require a JNK signal (13, 24), and as a consequence of this association CD95-tyrosine phosphorylation and formation of the death-inducing signaling complex occurred (Fig. 6*B*). EGFR/CD95 association was only induced upon TLCS/CHX coadministration but not with TLCS or CHX alone (Figs. 6*B* and 7*A*). The JNK inhibitory peptide could block the TLCS/CHX-induced CD95/EGFR association (Fig. 7*A*), indicating that the action of CHX in this respect is to provide a JNK signal.

CD95L was recently reported to prevent CD95-mediated apoptosis of quiescent HSC by induction of CD95-tyrosine nitration (Fig. 6*B*) (13, 25). No CD95-tyrosine nitration was observed in response to TLCS and/or CHX (Figs. 6*B* and 7*A*). However, CD95-tyrosine phosphorylation occurred in response to TLCS/CHX, which is required for the recruitment of FADD and caspase 8 to the CD95 (*i.e.* DISC formation; Figs. 6*B* and 7*A*) (6, 12). In line with these findings, coadministration of CD95L was able to inhibit TLCS/CHX-induced CD95-tyrosine phosphorylation and subsequent DISC formation by introducing a CD95-tyrosine nitration in quiescent HSC, but not in activated HSC (Fig. 7*B*). Therefore, and in line with Fig. 5*A*, CD95L inhibits TLCS/CHX-induced apoptosis in quiescent HSC only.

The pro-apoptotic effect of TLCS/CHX coadministration was largely abolished when TLCS-induced EGFR activation was prevented by inhibitors of sphingomyelinases, PKCζ, NADPH oxidases, Yes, or EGFR-tyrosine kinase activity by AY9944, PKCζ inhibitory pseudosubstrate, apocynin, SU6656, or AG1478, (Fig. 5*B*). Inhibition of JNK by L-JNKI-1, but not of Erk1/2 by PD 098059, also inhibited TLCS/CHX-induced apoptosis (Fig. 5*B*). These findings indicate that TLCS-induced EGFR activation can result in either HSC proliferation or apoptosis depending upon the signaling context. Interestingly, maneuvers which largely abolished DISC formation, *i.e.* SU6656, L-JNKI-1 and AG1478 (Fig. 7*A*), only approximately halved the number of apoptotic cells with respect to positive TUNEL staining (Fig. 5*B*). Thus, DISC-independent apoptotic pathways may also be involved, as reported recently for caspase-independent ROS-mediated apoptotic cell death (26). In hepatocytes, during lipoapoptosis a ROS-dependent but DISC-independent activation of the pro-apoptotic Bcl-2-family proteins Bim and Bax occurs, which then triggers the mitochondrial apoptotic pathway (27).

In support of our hypothesis that JNK signals are crucial for the switch from proliferation to apoptosis in response to TLCS, TLCS was coadministered with hydrogen peroxide, a known JNK activator. As shown in Fig. 8*A*, H_2O_2, but not TLCS alone, induced JNK1/2 phosphorylation. Both compounds, when given separately, did not activate CD95. However, coadministration of TLCS and H_2O_2 resulted not only in an activation of JNKs, but also induced EGFR/CD95 association, CD95-tyrosine phosphorylation, DISC formation (Fig. 8, *A* and *B*), and apoptosis (Fig. 8*C*). As shown in Fig. 8*B*, with TLCS present, low concentrations of H_20_2 (0.1 μM) did not induce JNK and CD95 activation, whereas H_2O_2 concentrations of 1 μM H_2O_2 and above induced JNK phosphorylation, CD95/EGFR association, CD95-tyrosine phosphorylation, and subsequent DISC formation (Fig. 8*C*). Thus, it is likely that critical amounts of ROS formation are required for JNK activation in quiescent HSC to couple bile acid-induced EGFR activation to CD95-mediated apoptotic signaling.

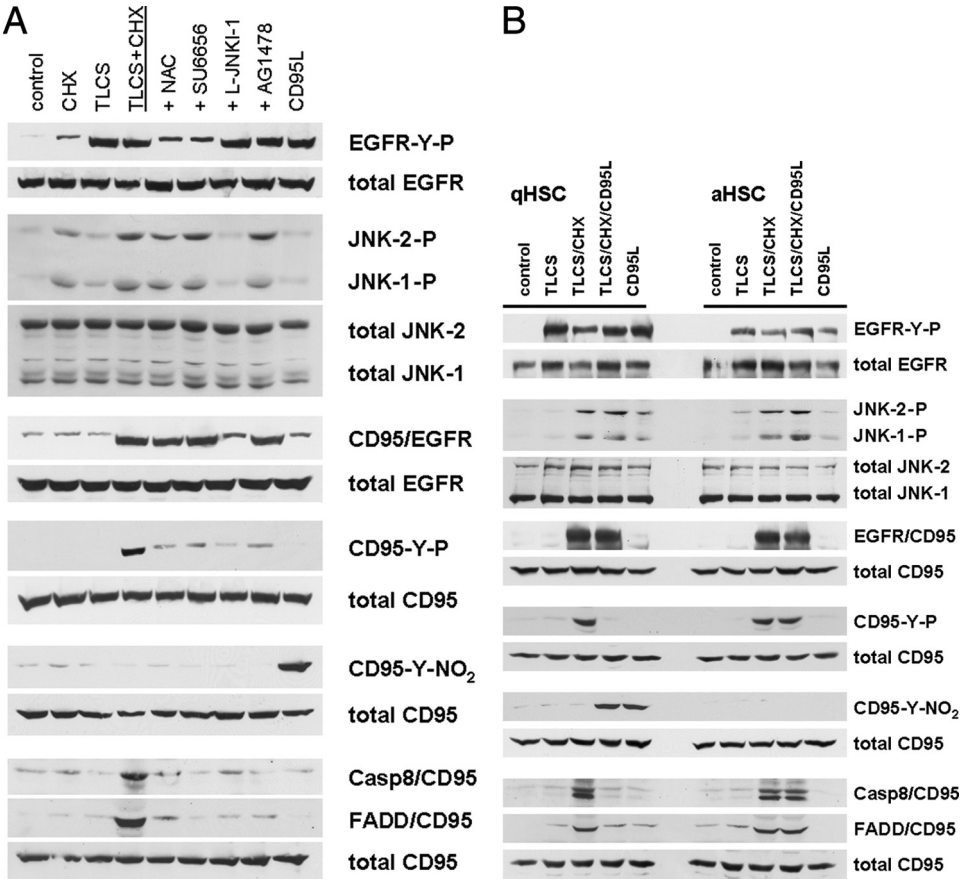

FIGURE 7. **JNK activation switches bile acid-induced EGFR activation toward CD95 activation and subsequent apoptosis in quiescent and activated HSC.** Quiescent (*A* and *B*) or activated HSC (*B*), respectively, were exposed to TLCS (100 μmol/liter), CHX (0.5 μmol/liter), CD95L (100 ng/ml), or TLCS/CHX or TLCS/CHX/CD95L was coadministered. When indicated, *N*-acetylcysteine (*NAC*, 30mmol/liter), SU6656 (10 μmol/liter), JNK inhibitor (L-JNKI-1, 5 μmol/liter) or AG1478 (5 μmol/liter) were added 30 min before TLCS/CHX were coadministration. Immunoprecipitation and Western blot analysis was performed as given in the legend to Fig. 6. *A*, inhibitor profile. In quiescent HSC, TLCS and CD95L induced EGFR phosphorylation but failed to induce a pronounced JNK1/2-signal, which is thought to be a prerequisite for CD95/EGFR association, and therefore, no CD95-tyrosine phosphorylation occurs. In addition, CD95L also induced a CD95-tyrosine nitration (13), which has been shown to prevent CD95-tyrosine phosphorylation and subsequent activation of the CD95 system (25), whereas no CD95-tyrosine nitration became detectable after TLCS treatment. Upon TLCS/CHX coadministration, a substantial JNK1/2 phosphorylation occurred which allowed for CD95/EGFR association. All maneuvers that prevented EGFR phosphorylation (*i.e. N*-acetylcysteine or SU6656), CD95/EGFR association (L-JNKI-1), or EGFR-tyrosine kinase activity (AG1478) also prevented TLCS/CHX-induced CD95-tyrosine phosphorylation, suggestive for an EGFR-mediated CD95-tyrosine phosphorylation and subsequent DISC formation, as has been previously reported in primary rat hepatocytes (6, 7). *B*, CD95L prevents TLCS/CHX-induced apoptosis in quiescent, but not in activated HSC. CD95L induced CD95-tyrosine nitration (13) and prevented TLCS/CHX-induced CD95-tyrosine phosphorylation and subsequent DISC formation in quiescent HSC. In activated HSC, however, no CD95-tyrosine nitration was triggered by CD95L, CD95-tyrosine phosphorylation was preserved, and CD95L did not inhibit TCLS/CHX-induced apoptosis (see Fig. 5*A*).

However, the question remains of why bile acids induce a sustained JNK activation in hepatocytes (6, 7), whereas in HSC, coadministration of either CHX or H_2O_2 is required to induce a JNK activation which is sufficient to switch proliferative EGFR activation toward CD95-mediated apoptotic signaling. Recently, a negative regulation of the MKK7-mediated JNK activation by the growth arrest and DNA damage-inducible gene (Gadd) 45β has been described for mouse hepatocytes (28), and in addition, NFκB-induced Gadd45β expression was reported to inhibit JNK-induced apoptosis by inhibiting the JKKK2/MKK7/JNK pathway (29). To our knowledge, Gadd45β expression in primary rat HSC has not been investigated so far. Indeed, mRNA and protein expression of Gadd45β in both quiescent and activated HSC was detected by PCR and Western blot, respectively, whereas only very little Gadd45β was detectable in primary rat hepatocytes (Fig. 9). Thus, a stronger expression of Gadd45β in HSC may counteract bile acid-induced JNK activation in HSC but not in hepatocytes.

In summary, in quiescent HSC bile acids act as a mitogenic and proliferative signal involving a NADPH oxidase-driven activation of the EGFR. This proliferative signal switches to a pro-apoptotic signal when a JNK1/2 signal, as induced by CHX or hydrogen peroxide, comes into play. Thus, JNKs act as a switch between proliferation and apoptosis.

DISCUSSION

Bile Acid-induced EGFR Phosphorylation and Proliferative Signaling in Quiescent Primary Rat Hepatic Stellate Cells—As shown in the present study, hydrophobic bile acids activate the EGFR in quiescent HSC through a NADPH oxidase-driven ROS formation and subsequent activation of the Src family kinase Yes. A similar mechanism has been reported for bile acid-induced EGFR activation in primary rat hepatocytes (6, 7, 23). In line with a ligand-independent EGFR activation by hydrophobic bile acids in HSC, EGFR became tyrosine-phosphorylated at positions 845 and 1173 but not at position 1045. However, phosphorylation of Tyr^{1045} occurs in response to exogenous EGF or CD95L-induced EGF shedding (13).

The inhibitor studies suggest that sphingomyelinases, PKCζ-mediated $p47^{phox}$ -serine phosphorylation, and activation of NADPH oxidases are upstream events of bile acid-induced EGFR activation. The resulting ROS response may then result in a Yes kinase-mediated EGFR transactivation. Therefore, the mechanism underlying bile acid-induced EGFR activation in HSC is similar to that described recently in detail in hepatocytes (7, 23).

Whereas in primary rat hepatocytes bile acid-induced EGFR activation is coupled to an activation of the CD95 system and thereby triggers apoptotic cell death (6, 7, 23), in quiescent HSC, bile acid-induced activation of the EGFR failed to induce apoptosis and even stimulated HSC proliferation. This may relate to recent reports which suggest that quiescent HSC rep-

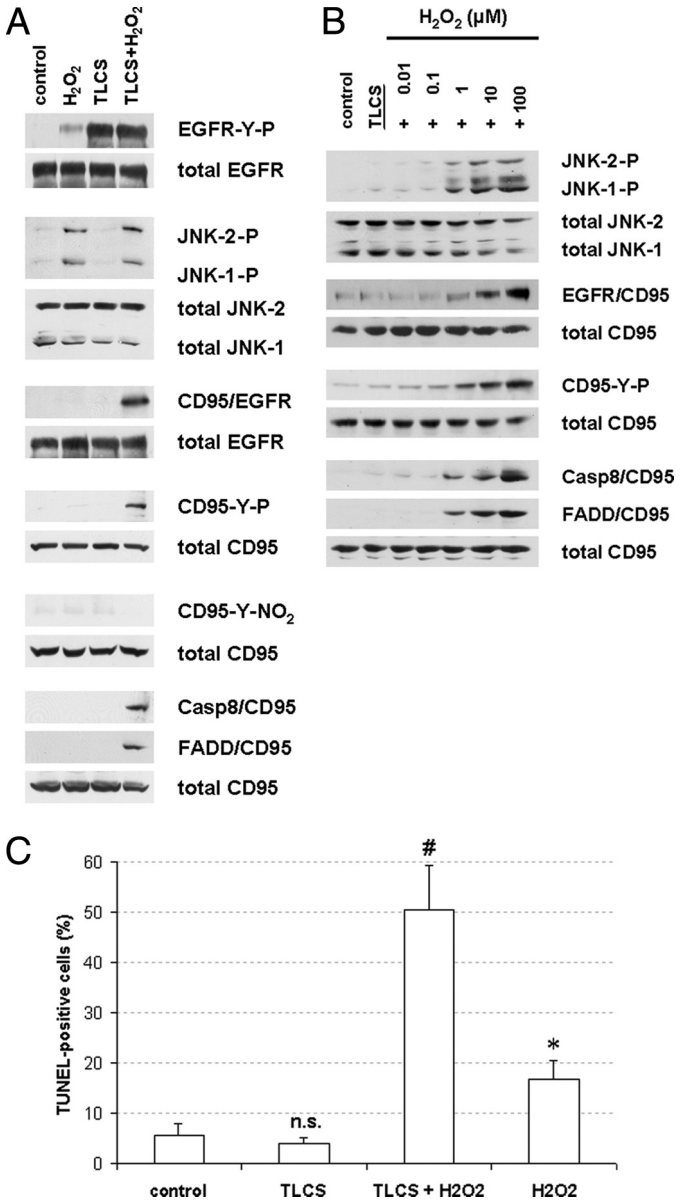

FIGURE 8. **Hydrogen peroxide-induced JNK activation couples bile acid-induced EGFR activation to CD95-mediated apoptosis.** Quiescent HSC were exposed to TLCS (100 μmol/liter) and hydrogen peroxide (H_2O_2, 100 μmol/liter), or TLCS/H_2O_2 were coadministered. Immunoprecipitation and Western blot analysis was performed as given in the legend to Fig. 6. TUNEL staining was performed as given under "Experimental Procedures." *A* and *B*, H_2O_2-induced JNK activation led to CD95/EGFR association, which was followed by CD95-tyrosine phosphorylation, DISC formation (*A*) and subsequent apoptosis as detected by TUNEL staining (*B*). Therefore, JNK activation switches TLCS-induced EGFR activation from proliferation to apoptosis. * denotes statistical significance compared with control ($p < 0.05$); # denotes statistical significance compared with TLCS alone ($p < 0.05$); *n.s.* (not significant, $p > 0.05$). *C*, dose response curve. H_2O_2 induced JNK phosphorylation starting at a dose of 1–10 μM in quiescent HSC, which resulted in CD95/EGFR association, CD95-tyrosine phosphorylation, and subsequent DISC formation.

resent a hepatic stem/progenitor cell compartment (14, 30, 31, 37).

This differential behavior may be of pathophysiological relevance in cholestatic liver disease. Here, high levels of hydrophobic bile acids on the one hand cause hepatocyte apoptosis but on the other induce regeneration because of proliferation of quiescent HSC.

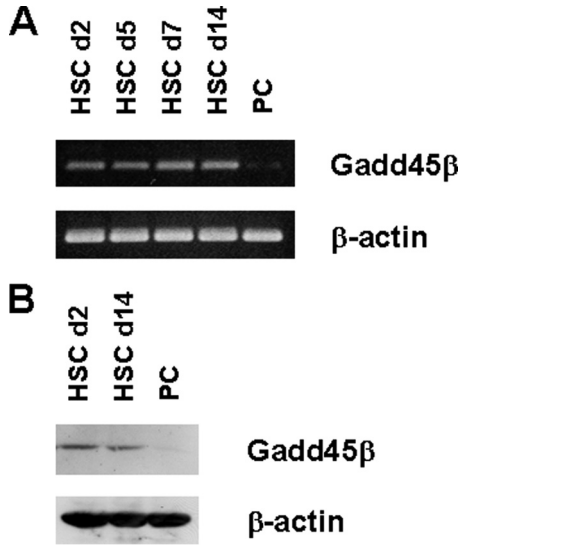

FIGURE 9. **Gadd45β expression in primary rat HSC and hepatocytes.** Primary rat hepatocytes (parenchymal cells (*PC*)) were isolated and cultured for 24 h as published recently (12). Primary rat HSC were cultured for 2–14 days as indicated. Then HSC and parenchymal cells were detected for Gadd45β-mRNA expression by reverse transcription-PCR (*A*) and for Gadd45β-protein expression by Western blot (*B*), respectively, as described under "Experimental Procedures." β-Actin served as a loading control.

JNKs Provide the Switch between Bile Acid-induced Proliferation and Apoptosis in HSC—In hepatocytes, bile acid-induced EGFR activation leads to CD95 activation in a JNK-dependent way, which finally results in apoptotic cell death (6, 7, 23).

However, in quiescent HSC, bile acid-induced EGFR activation increases cell proliferation. This may be explained by the fact that hydrophobic bile acids failed to induce JNK activation in HSC despite induction of a NADPH oxidase-driven ROS-response, which in hepatocytes, but not in HSC, triggers JNK activation (6, 7, 23). The reason for this difference remains unclear but may relate to the intensity of bile acid-induced ROS formation. In line with this, the addition of hydrogen peroxide was able to induce JNK activation in quiescent HSC. Furthermore, there may be cell type-specific differences in ROS-dependent JNK activation (33), which may involve inhibition of JNK-inactivating phosphatases (MKP1, -3, -5, and -7) (34), ROS-dependent activation of the apoptosis signal-regulating kinase 1, which can trigger MKK4/7-mediated JNK activation (33), or Gadd45β-dependent mechanisms (28). Tumor necrosis factor α-induced ROS formation was shown to inhibit JNK-inactivating phosphatases (MKP-1, -3, -5, and -7) by converting their catalytic cysteine to sulfenic acid, resulting in a sustained JNK activation (34). In addition, ROS-dependent activation of the apoptosis signal-regulating kinase 1, leading to a MKK4/7-mediated JNK activation, has also been described (33). Thus, one possible explanation for the observed lack in bile acid-induced JNK activation in primary rat HSC compared with hepatocytes could be a lack of apoptosis signal-regulating kinase 1 expression in those cells. High amounts of ROS, *e.g.* by exogenous hydrogen peroxide addition, would then overcome this situation via inhibition of JNK-inactivating phosphatases. Finally, a negative regulation of the MKK7-mediated JNK activation by Gadd45β might be an alternative explanation (29), as an increased expression of Gadd45β in HSC would inhibit bile

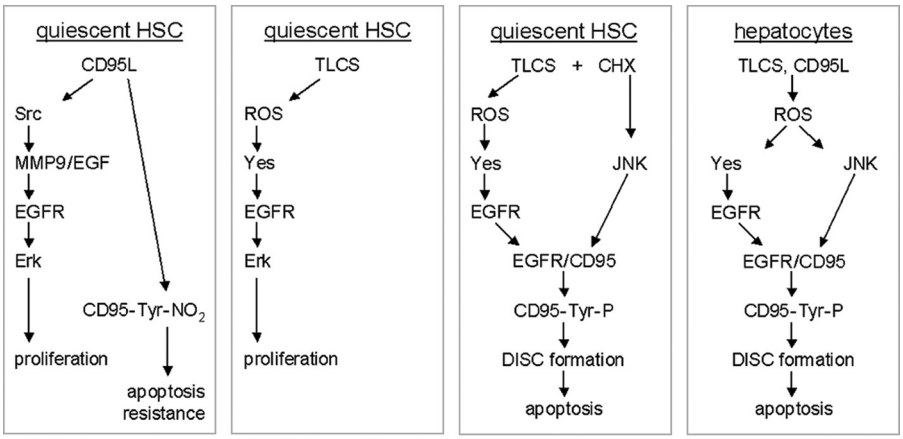

FIGURE 10. **Bile acid- and CD95L-induced proliferation and apoptosis in quiescent HSC and hepatocytes.** This figure summarizes our current view on pro-apoptotic bile acid-, *i.e.* TLCS, and CD95L-induced signaling in primary rat quiescent HSC and hepatocytes. In hepatocytes both, CD95L and the pro-apoptotic bile acid TLCS led to an instantaneous ROS generation which has two functional consequences, activation of the Src-family kinase Yes and the mitogen-activated protein kinase JNK (6, 7, 12). Whereas Yes then transactivates the EGFR, JNK activation induces CD95/EGFR association, which is crucial for EGFR-mediated CD95-tyrosine phosphorylation, DISC formation, and apoptosis (6, 7, 12). In quiescent HSC, CD95L induced a rapid CD95-tyrosine nitration (13) and thereby resistance toward CD95-mediated apoptosis (13, 25). In addition, CD95L mediates Src- and MMP9-dependent EGF-shedding and subsequent ligand-dependent EGFR activation and Erk-dependent proliferation (13). In contrast, TLCS induced ROS-dependent Yes activation and subsequent Yes-mediated EGFR transactivation, resulting in an Erk-dependent HSC proliferation. However, upon induction of a substantial JNK activation by either CHX or hydrogen peroxide, CD95/EGFR association occurred, resulting in an EGFR-mediated CD95-tyrosine phosphorylation, DISC formation, and apoptosis (this study).

acid-induced JNK activation. As shown in this study, Gadd45β expression is higher in primary rat HSC compared with primary rat hepatocytes. Therefore, Gadd45β might suppress bile acid-induced JNK activation via a negative MKK7 regulation (29). Further studies are required to settle this issue.

Activation of JNK in liver parenchymal cells or whole liver lysates upon liver injury has been reported to occur *in vivo* in models of dietary obesity, toxin-mediated tumor necrosis factor-dependent liver injury, and acetaminophen intoxication (for review, see Ref. 26). Here, JNK activation was shown to depend on death receptors, endoplasmic reticulum stress, and caspase-independent ROS-mediated cell death (26). JNK activation in rat HSC has been recently shown in two *in vivo* models of liver injury, *i.e.* dimethylnitrosamine administration and bile duct ligation (35). Interestingly, dimethylnitrosamine administration was much more potent than bile duct ligation in order to induce JNK phosphorylation in HSC, and it was suggested that this difference is because of a greater ability of dimethylnitrosamine administration to induce ROS formation compared with bile duct ligation (35). Therefore, cholestasis *per se* may favor HSC proliferation because of subcritical JNK activation, whereas a "second hit" like free fatty acids, inflammation/toxin-mediated liver injury, or other conditions leading to a pronounced ROS generation and subsequent sustained JNK activation may switch proliferative signaling toward apoptotic signaling. This may be of pathophysiological relevance in view of the reported role of HSC as liver stem/progenitor cells (14).

Similar to hydrogen peroxide, CHX also induced significant JNK activation in quiescent HSC, which was sufficient to shift bile acid-induced EGFR activation away from proliferation toward CD95-mediated apoptosis by allowing for JNK-dependent CD95/EGFR association and subsequent EGFR-mediated CD95-tyrosine phosphorylation. In line with this, a JNK inhibitor shifted TLCS-induced HSC apoptosis in the presence of CHX back to a proliferative signal. Furthermore, all maneuvers which prevented bile acid-induced EGFR activation inhibited both TLCS-induced quiescent HSC proliferation and TLCS/CHX-induced quiescent HSC apoptosis, suggesting that bile acid-induced EGFR activation is crucial for both proliferation and apoptosis, whereas JNK-signals determine the outcome.

The addition of CD95L in quiescent HSC also leads to an activation of the EGFR, which, however, is induced by a Src- and MMP9-dependent shedding of EGF and subsequent ligand-dependent EGFR activation (13). CD95L also failed to induce a sustained JNK activation in HSC (13, 24), whereas CD95L is a known JNK activator in hepatocytes (12). In activated HSC, coadministration of CD95L/CHX induced apoptosis but not in quiescent HSC. This was shown to be because of a CD95L-induced CD95-tyrosine nitration (13), which inactivates the CD95 (25). Such a CD95-tyrosine nitration was not observed in response to hydrophobic bile acids, rendering quiescent HSC potentially susceptible toward bile acid-induced apoptosis. Fig. 10 summarizes our current view on pro-apoptotic bile acid- and CD95L-induced signaling in quiescent HSC and hepatocytes, respectively.

In conclusion, in quiescent HSC, hydrophobic bile acids activate the EGFR, and this can couple to both cell proliferation and apoptosis, depending on the JNK signaling. Therefore, JNK act as a switch between bile acid-induced proliferation and apoptosis in HSC. This may offer new therapeutic perspectives in cholestatic liver disease, especially in view of the proposed role of quiescent HSC as a stem/progenitor cell compartment.

REFERENCES

1. Chieco, P., Romagnoli, E., Aicardi, G., Suozzi, A., Forti, G. C., and Roda, A. (1997) *Histochem. J.* **29,** 875–883
2. Faubion, W. A., Guicciardi, M. E., Miyoshi, H., Bronk, S. F., Roberts, P. J., Svingen, P. A., Kaufmann, S. H., and Gores, G. J. (1999) *J. Clin. Invest.* **103,** 137–145
3. Miyoshi, H., Rust, C., Roberts, P. J., Burgart, L. J., and Gores, G. J. (1999) *Gastroenterology* **117,** 669–677
4. Yerushalmi, B., Dahl, R., Devereaux, M. W., Gumpricht, E., and Sokol, R. J. (2001) *Hepatology* **33,** 616–626
5. Graf, D., Kurz, A. K., Fischer, R., Reinehr, R., and Häussinger, D. (2002) *Gastroenterology* **122,** 1411–1427
6. Reinehr, R., Graf, D., and Häussinger, D. (2003) *Gastroenterology* **125,** 839–853
7. Reinehr, R., Becker, S., Wettstein, M., and Häussinger D. (2004) *Gastroenterology* **127,** 1540–1557
8. Werneburg, N. W., Yoon, J. H., Higuchi, H., and Gores, G. J. (2003) *Am. J. Physiol. Gastrointest. Liver Physiol.* **285,** G31–G36
9. Svegliati-Baroni, G., Ridolfi, F., Hannivoort, R., Saccomanno, S., Homan,

M., De Minicis, S., Jansen, P. L., Candelaresi, C., Benedetti, A., and Moshage, H. (2005) *Gastroenterology* **128,** 1042–1055
10. Galle, P. R., Hofmann, W. J., Walczak, H., Schaller, H., Otto, G., Stremmel, W., Krammer, P. H., and Runkel, L. (1995) *J. Exp. Med.* **182,** 1223–1230
11. Kondo, T., Suda, T., Fukuyama, H., Adachi, M., and Nagata, S. (1997) *Nat. Med.* **3,** 409–413
12. Reinehr, R., Schliess, F., and Häussinger, D. (2003) *FASEB J.* **17,** 731–733
13. Reinehr, R., Sommerfeld, A., and Häussinger, D. (2008) *Gastroenterology* **134,** 1494–1506
14. Kordes, C., Sawitza, I., Müller-Marbach, A., Ale-Agha, N., Keitel, V., Klonowski-Stumpe, H., and Häussinger, D. (2007) *Biochem. Biophys. Res. Commun.* **352,** 410–417
15. Fischer, R., Cariers, A., Reinehr, R., and Häussinger, D. (2002) *Gastroenterology* **123,** 845–861
16. Bataller, R., Schwabe, R. F., Choi, Y. H., Yang, L., Paik, Y. H., Lindquist, J., Qian, T., Schoonhoven, R., Hagedorn, C. H., Lemasters, J. J., and Brenner, D. A. (2003) *J. Clin. Invest.* **112,** 1383–1394
17. Piiper, A., Elez, R., You, S. J., Kronenberger, B., Loitsch, S., Roche, S., and Zeuzem, S. (2003) *J. Biol. Chem.* **278,** 7065–7072
18. Friedman, S. L. (1993) *N. Engl. J. Med.* **328,** 1828–1835
19. Pinzani, M. (1995) *J. Hepatol.* **22,** 700–706
20. Gressner, A. M. (1998) *Cell Tissue Res.* **292,** 447–452
21. Biscardi, J. S., Maa, M. C., Tice, D. A., Cox, M. E., Leu, T. H., and Parsons, S. J. (1999) *J. Biol. Chem.* **274,** 8335–8343
22. Poppleton, H. M., Wiepz, G. J., Bertics, P. J., and Patel, T. B. (1999) *Arch. Biochem. Biophys.* **363,** 227–236
23. Reinehr, R., Becker, S., Keitel, V., Eberle, A., Grether-Beck, S., and Häussinger, D. (2005) *Gastroenterology* **129,** 2009–2031
24. Cariers, A., Reinehr, R., Fischer, R., Warskulat, U., and Häussinger, D. (2002) *Cell. Physiol. Biochem.* **12,** 179–186
25. Reinehr, R., Görg, B., Höngen, A., and Häussinger, D. (2004) *J. Biol. Chem.* **279,** 10364–10373
26. Malhi, H., and Gores, G. J. (2008) *Gastroenterology* **134,** 1641–1654
27. Malhi, H., Bronk, S. F., Werneburg, N. W., and Gores, G. J. (2006) *J. Biol. Chem.* **281,** 12093–12101
28. Papa, S., Monti, S. M., Vitale, R. M., Bubici, C., Jayawardena, S., Alvarez, K., De Smaele, E., Dathan, N., Pedone, C., Ruvo, M., and Franzoso, G. (2007) *J. Biol. Chem.* **282,** 19029–19041
29. Papa, S., Zazzeroni, F., Bubici, C., Jayawardena, S., Alvarez, K., Matsuda, S., Nguyen, D. U., Pham, C. G., Nelsbach, A. H., Melis, T., De Smaele, E., Tang, W. J., D'Adamio, L., and Franzoso, G. (2004) *Nat. Cell Biol.* **6,** 146–153
30. Sicklick, J. K., Choi, S. S., Bustamante, M., McCall, S. J., Pérez, E. H., Huang, J., Li, Y. X., Rojkind, M., and Diehl, A. M. (2006) *Am. J. Physiol. Gastrointest. Liver Physiol.* **291,** G575–G583
31. Yang, L., Jung, Y., Omenetti, A., Witek, R. P., Choi, S., Vandongen, H. M., Huang, J., Alpini, G. D., and Diehl, A. M. (2008) *Stem Cells* **26,** 2104–2113
32. Levitzki, A., and Gazit, A. (1995) *Science* **267,** 1782–1788
33. Schwabe, R. F., and Brenner, D. A. (2006) *Am. J. Physiol. Gastrointest. Liver Physiol.* **290,** G583-G589
34. Kamata, H., Honda, S., Maeda, S., Chang, L., Hirata, H., and Karin, M. (2005) *Cell* **120,** 649–661
35. Svegliati-Baroni, G., Ridolfi, F., Caradonna, Z., Alvaro, D., Marzioni, M., Saccomanno, S., Candelaresi, C., Trozzi, L., Macarri, G., Benedetti, A., and Folli, F. (2003) *J. Hepatol.* **39,** 528–537
36. Blake, R. A., Broome, M. A., Liu, X., Wu, J., Gishizky, M., Sun, L., and Courtneidge, S. A. (2000) *Mol. Cell. Biol.* **20,** 9018–9027
37. Sawitza, I., Kordes, C., Reister, S., and Häussinger, D. (2009) *Hepatology*, in press